Effects of Mg and Cu Dopants on the Properties of Zinc Oxide Nanorod Arrays

M.F. Malek[1,2,*], M.H. Mamat[3], A.S. Ismail[3], R. Mohamed[3,4], M.J. Salifairus[1,2], Z. Khusaimi[1,2], and M. Rusop[1,3]

Abstract - **We had successfully synthesised Mg-doped zinc oxide (MZO) and Cu-doped zinc oxide (CZO) nanorod arrays (NRAs) on Al-doped ZnO (ZAO)-coated glass substrates using immersion method and investigated their structural properties. With the incorporation of the Mg dopant, the length and crystallinity of MZO NRAs is higher compared to that of the CZO NRAs. The average optical transmittance of MZO NRAs was slightly lower than that of the CZO NRAs over the visible wavelength region. With the incorporation of the Cu dopant, the morphology of the CZO sample was slightly different from that of the MZO NRAs. The CZO NRAs present granular with small sphere shape. On the other hand, the MZO NRAs exhibit a hexagonal shape structure with a flat-top facet. Rods with a diameter of 58.9-96.7 nm were uniformly grown on the ZAO-coated glass substrate. This paper presents the growth behaviors of the MZO and CZO NRAs.**

Keywords - ZnO; Dopant; Nanorods; Mg; Cu

[1] NANO-SciTech Centre (NST), Institute of Science (IOS), Universiti Teknologi MARA (UiTM), 40450 Shah Alam, Selangor, Malaysia
[2] Faculty of Applied Sciences, Universiti Teknologi MARA (UiTM), 40450 Shah Alam, Selangor, Malaysia
[3] NANO-ElecTronic Centre (NET), Faculty of Electrical Engineering, Universiti Teknologi MARA (UiTM), 40450 Shah Alam, Selangor, Malaysia
[4] Faculty of Applied Sciences, Universiti Teknologi MARA (UiTM), Cawangan Pahang Kampus Jengka, 26400 Bandar Tun Abdul Razak Jengka,
Pahang, Malaysia

✉ M.F. Malek
*mfmalek07@uitm.edu.my; mfmalek07@gmail.com

Received : 23 November 2017
Accepted : 31 December 2017
Published : 31 December 2017

I. INTRODUCTION

ZnO nanorod arrays (NRAs) are attracting the attention of many researchers because of their unique and enhanced properties thereby offering numerous potential applications such as light-emitting diodes (LEDs), solar cells and sensors. ZnO has a large exciton binding energy (60 meV) with a wide direct band gap (3.37 eV) at room temperature, abundance in nature, non-toxicity, high thermal and chemical stability. The properties of ZnO can be tuned, which is important to achieve the considerable applications and doping process has been proved to be one of the alternative. Various elements such as Cu, Al, Fe, Ni, Er, Mg, and Mn, have been used to dope ZnO [1, 2]. Among the elements, Mg and Cu has been identified as an attractive doping element because of the similarity of the ionic radius of Mg^{2+} (0.72 Å), Cu^{+} (0.77 Å) and Cu^{2+} (0.73 Å) with Zn^{2+} (0.74 Å), which means that replacing Zn with Mg and Cu will not induce any phase transition or lattice distortion. This will reduce or eliminate the formation of native defects causing from nonstoichiometric property of ZnO nanostructure. Various techniques, such as pulse laser deposition (PLD) [3], metal–organic chemical vapor deposition (MOCVD), electrochemical deposition [4], thermal evaporation [5], spray pyrolysis [6] and radio frequency (RF) reactive magnetron sputtering [7, 8] have been used

for the growth of ZnO-based NRs which usually require complex synthesis setup or high temperature and harmful solvents. Among all the techniques, immersion technique is known as a versatile, low cost, requires low temperature, easy control of deposition parameters, simple deposition set-up and great potential for scale-up. In our previous study, we reported the properties of ZnO NRs grown on an Al-doped ZnO (ZAO) seed layer using immersion methods [9]. In this study, we grew Mg-doped ZnO (MZO) and Cu-doped ZnO (CZO) NRAs on ZnO seed layers that were prepared on ZAO-coated glass substrates. We hope our work can shed new light on the synthesisation of ZnO-based materials.

II. MATERIALS AND METHOD

MZO and CZO NRAs were grown via immersion process. ZAO seed layer thin films were deposited on the glass substrates by sol-gel dip-coating technique. Then, the MZO and CZO NRAs were grown on the top of seed crystal layer using immersion technique. An aqueous solutions of 0.1 M zinc nitrate hexahydrate [$Zn(NO_3)_2.6H_2O$] and 0.1 M hexamethylenetetramine [HMT; $C_6H_{12}N_4$] were used as a precursor and stabiliser, respectively. It is aimed to obtain 1 at.%. of doped ZnO thin films solution with magnesium and copper using $Mg(NO_3)_2.6H_2O$ and $Cu(NO_3)_2.2.5H_2O$ compounds, respectively. All the reagents were dissolved and reacted in a beaker filled with distilled water as a solvent under ultrasonic irradiation at 50 ºC for 30 min. Next, the solution was stirred and aged for 3 h at room temperature. The resulting solution was poured into a vessel which contained the seed layer-coated glass substrates. Next, the samples were immersed at 95 ºC for 50 min. Finally, the samples were annealed in a furnace at 500 ºC for 1 h. The crystal structures properties and phases of the MZO and CZO NRAs were investigated using an X-ray diffractometer (XRD, model: Bruker AXS D8 Advance). The surface morphology and thicknesses of the films were observed by Field Emission Scanning Electron Microscopy (FESEM, model: JEOL JSM 7600F).

III. RESULTS AND DISCUSSION

The XRD patterns of MZO and CZO NRAs are shown in Fig. 1. All diffraction peaks belong to the (100), (002), (101) and (102) planes of hexagonal wurtzite ZnO phase (JCPDS card No. 36-1451). There are no other impurity peaks are observed, indicating no secondary phase in both samples. It is well known that the crystal growth occurs along the plane with the lowest surface energy. In wurtzite ZnO crystals, (002) plane has the lowest surface energy, thus both MZO and CZO NRAs show the strongest diffraction peak corresponding to the (002) plane [10, 11]. It is noted that the intensity of (002) peak for MZO is higher than CZO. This may because the Mg atoms easily substituted Zn atoms in the lattice, and yielded better crystallinity and *c*-axis orientation [12].

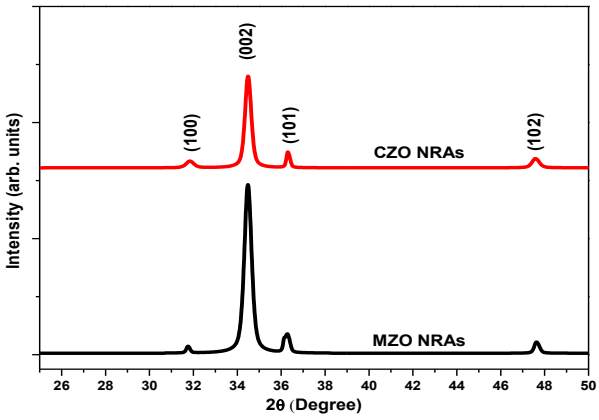

Fig. 1. XRD patterns of MZO and CZO NRAs grown via immersion technique

Fig. 2 (a) shows the top view FESEM image of the MZO NRAs (30 k magnification at 5 kV applied voltage). The variation in the diameter of the NRAs can be explained by the ionic radii of Mg^{2+} (0.53 Å) and Cu^{2+} (0.73 Å) which is smaller or almost similar than that of Zn^{2+} (0.74 Å) and that of

Cu^{+} (0.77 Å) which is bigger than that of Zn^{2+} [13, 14]. The diameter size of the NRAs could be estimated by different dopants during the deposition process where the doping process might occur by interstitial and/or substitution reaction. The MZO NRAs are uniformly grown on the surface of the seed layer and aligned perpendicular to the ZAO-coated glass substrate. The average diameter of the NRs is 96.7 nm. The top view FESEM image of CZO NRAs is shown in Fig. 2 (b). With the incorporation of the Cu dopant, the average diameter is smaller compared to MZO NRAs with granular and spherical morphologies. The average values of the diameter, length and aspect ratio of the MZO and CZO NRAs are summarised in Table 1. High aspect ratio represents a large surface area which might introduce novel properties, high electron mobility and quantum confinement effects. The growing mechanism of the MZO and CZO NRAs using zinc nitrate, HMT and dopant sources can be proposed in the following equations [15, 16]:

$$Zn(NO_3)_2 + C_6H_{12}N_4 \rightarrow [Zn(C_6H_{12}N_4)]^{2+} + 2NO_3^- \quad \ldots(1)$$

$$C_6H_{12}N_4 + 6H_2O \leftrightarrow 4NH_3 + 6CH_2O \quad \ldots(2)$$

$$NH_3 + H_2O \leftrightarrow NH_4^+ + OH^- \quad \ldots(3)$$

$$C_6H_{12}N_4 + Zn^+ \rightarrow [Zn(C_6H_{12}N_4)]^{2+} \quad \ldots(4)$$

$$Zn^{2+} + 4OH^- \rightarrow Zn(OH)_4^{2-} \quad \ldots(5)$$

$$[Zn(C_6H_{12}N_4)]^{2+} + 2OH^- \rightarrow ZnO + H_2O + C_6H_{12}N_4 \quad \ldots(6)$$

$$Zn^{2+} + 2OH^- \leftrightarrow ZnO + H_2O \quad \ldots(7)$$

or

$$Zn^{2+} + 2OH^- \leftrightarrow Zn(OH)_2 \leftrightarrow ZnO + H_2O \quad \ldots(8)$$

For MZO:

$$Mg(NO_3)_2.6H_2O \rightarrow Mg^{2+} + 2NO_3^- + 6H_2O \quad \ldots(9)$$

$$2Mg^{2+} + 4OH^- \rightarrow 2MgO + 2H_2O \quad \ldots(10)$$

For CZO:

$$Cu(NO_3)_2 2.5H_2O \rightarrow Cu^{2+} + 2NO_3^- + 2.5H_2O \quad \ldots(11)$$

$$2Cu^{2+} + 4OH^- \rightarrow 2CuO + 2H_2O \quad \ldots(12)$$

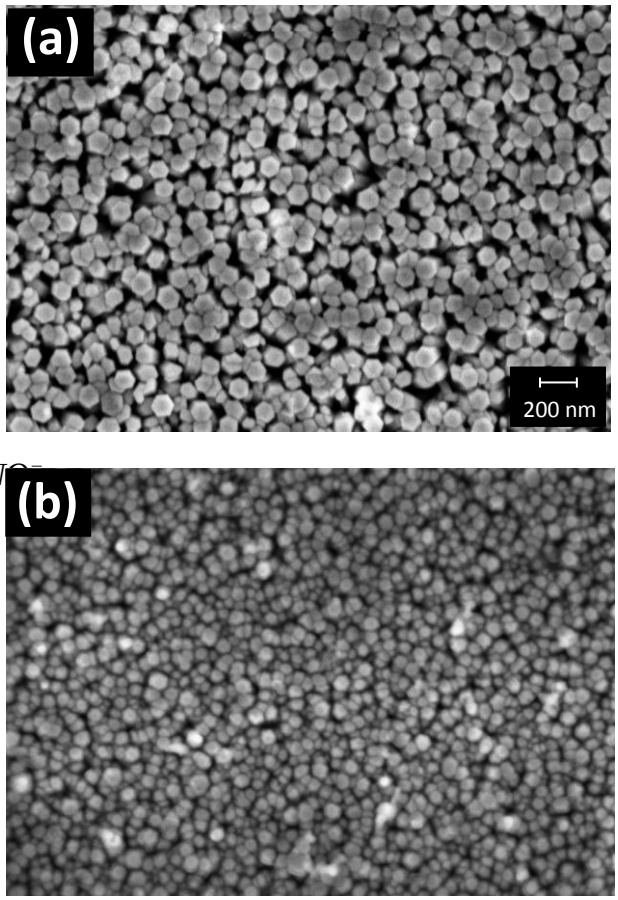

Fig. 2. Top view FESEM images of (a) MZO and (b) CZO NRAs

Table 1: Average diameter, length and aspect ratio of MZO and CZO NRAs

Samples	Average diameter (nm)	Length (nm)	Aspect ratio	Average transmittance (%)
MZO	96.7	642	6.6	83.85
CZO	58.9	300	5.1	95.48

HMT is first decomposed to ammonia (NH_3) and formaldehyde (CH_2O), which generates OH^- ions by the reaction with H_2O [17]. Besides, HMT also forms the $[Zn(C_6H_{12}N_4)]^{2+}$ complex through the reaction with Zn^{2+} ions that enhance the growth process of the nanorods [18]. On the other hand, $Zn(OH)_2$ complexes were formed through the reaction between Zn^{2+} with readily OH^- ions which act as the growth unit for the ZnO NRAs. Finally, the formation of ZnO NRAs was obtained from the decomposition of $Zn(OH)_2$. In addition, HMT also plays an important role during the deposition process where OH^- ions were being supplied to Zn^{2+}, Mg^{2+} and Cu^{2+} to form Zn-O, Mg-O and Cu-O bonds here, respectively. Thereby, doping of the ZnO lattice was achieved by interstitial and/or substitution reaction. Vertically well-aligned NRs plays a vital role in the fabrication of nanoscale electronics and optoelectronics.

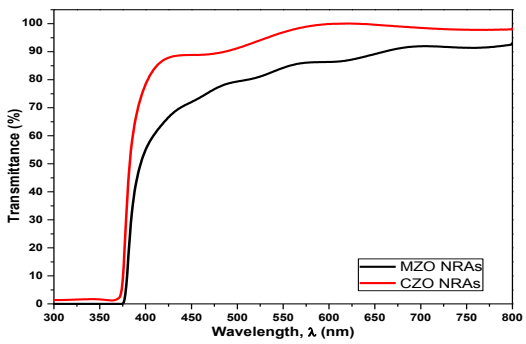

Fig. 3. Transmittance spectra of MZO and CZO NRAs

Fig. 3 shows the optical transmittance spectra of the MZO and CZO NRAs within the range between 300 and 800 nm. Both of the NRAs exhibit higher transmission properties of above 83 % in the visible light region and in agreement with the previous measured length of the structure. In comparison to the MZO, the CZO NRAs exhibited significantly higher transmittance which due to thin layer film. The variation in the absorption edges can be clearly observed which might due to the difference size in ionic radius between the impurities ions that cause the light scattering effects in the NRAs structures [19, 20]. From the data analysis, the highest average transmittance in the visible region was achieved for the CZO NRAs which is 95.48 %. On the other hand, the lowest transmittance of 83.85 % was obtained for the sample doped with magnesium on the same wavelength.

IV. CONCLUSIONS

We investigated the structural properties of MZO and CZO NRAs grown on the ZAO-coated glass substrate. The Mg and Cu dopants had affect the growth behavior of the ZnO NRAs.

A long and well-aligned NRAs with high crystallinity was achieved by incorporating the Mg dopant. By contrast, the addition of the Cu dopant induced significant morphological changes in the NRAs. It is also observed that the average transmittance of the NRAs is reduced with the length/thickness increment. It can be concluded that the growth behaviors of ZnO NRs can be controlled by choosing suitable dopant agent.

ACKNOWLEDGMENTS

The authors would like to thank the Microelectronic and Nanotechnology – Shamsuddin Research Centre (MiNT-SRC), Universiti Tun Hussein Onn (UTHM) for the use of their XRD facility. The authors thank Mr. Mohd Azlan Jaafar (UiTM assistant engineer), Mr. Mohd Suhaimi

Ahmad (UiTM assistant engineer) and Mrs. Nurul Wahida (UiTM Asst. Science Officer) for their kind support of this research.

REFERENCES

[1] de Almeida, V. M.; Mesquita, A.; de Zevallos, A. O.; Mamani, N. C.; Neves, P. P.; Gratens, X.; Chitta, V. A.; Ferraz, W. B.; Doriguetto, A. C.; Sabioni, A. C. S. and de Carvalho, H. B.; 2007: J. Alloys Compd 655 : 406 – 414.

[2] Sun, L.; Lin, Z.; Zhou, X.; Zhang, Y. and Guo, T.; 2016: J. Alloys Compd 671 : 473 – 478.

[3] Shewale, P. S. and Yu, Y. S.; 2016: J. Alloys Compd 654 : 79 – 86.

[4] Henni, A.; Merrouche, A.; Telli, L. and Karar, A.; 2016: J. Electroanal. Chem 763 : 149 – 154.

[5] Kyaw, A. K. K.; Sun, X. W.; Jiang, C. Y.; Lo, G. Q.; Zhao, D. W. and Kwong, D. L.; 2008: Appl. Phys. Lett 93 : 221107.

[6] Kulandaisamy, A. J.; Reddy, J. R.; Srinivasan, P.; Babu, K. J. Mani, G. K.; Shankar, P. and Rayappan, J. B. B.; 2006: J. Alloys Compd 688 : 422 – 429.

[7] Sreedhar, A.; Kwon, J. H.; Yi, J.; Kim, J. S. and Gwag, J. S.; 2016: Mater. Sci. Semicond. Process 49 : 8 – 14.

[8] Ghafouri, V.; Shariati, M. and Ebrahimzad, A.; 2012: Scientia Iranica 19 : 934 – 942.

[9] Malek, M. F.; Mamat, M. H.; Soga, T.; Rahman, S. A.; Bakar, S. A.; Ismail, A. S.; Mohamed, R.; Alrokayan, S. A. H.; Khan, H. A. and Mahmood, M. R.; 2016: Jpn J. Appl. Phys 55 : 1 – 15.

[10] Xu, L.; Li, X.; Chen, Y. and Xu, F.; 2011: Appl. Surf. Sci 257 : 4031 – 4037.

[11] Fujimara, N.; Nishibara, T.; Goto, S.; Xu, J. and Ito, T.; 1993: J. Cryst. Growth 130 : 269 – 279.

[12] Kang, H. S.; Kim, G. H.; Lim, S. H.; Chang, H. W.; Kim, J. H. and Lee, S.Y.; 2008: Thin Solid Films 516 : 3147 – 3149.

[13] Al Asmar, R.; Juillaguet, S.; Ramonda, M.; Giani, A.; Combette, P.; Khoury, A. and Foucaran, A.; 2005: J. Cryst. Growth 275 : 512 – 520.

[14] Azimirad, R.; Khayatian, A.; Safa, S. and Almasi Kashi, M.; 2014: J. Alloys Compd 615 : 227 – 233.

[15] Lupan, O.; Chow, L.; Chai, G.; Roldan, B.; Naitabdi, A.; Schulte, A. and Heinrich, H.; 2007: Mater. Sci. Eng. B 145 : 57 – 66.

[16] Sun, Y.; Riley, D. J. and Ashfold, M. N. R.; 2006: J. Phys. Chem. B 110 : 15186 – 15192.

[17] Malek, M. F.; Sahdan, M. Z.; Mamat, M. H.; Musa, M. Z.; Khusaimi, Z.; Husairi, S. S.; Md Sin, N. D. and Rusop, M.; 2013: Appl. Surf. Sci 275 : 75 – 83.

[18] Ahsanulhaq, Q.; Umar, A. and Hahn, Y. B.; 2007: Nanotechnology 18 : 115603.

[19] Yung, K. C.; Liem, H. and Choy, H. S.; 2009: J. Phys. D 42:185002.

[20] Yadav, R. S.; Mishra, P. and Pandey, A. C.; 2008: Ultrason. Sonochem 15 : 863 – 868.